2011 American Control Conference
on O'Farrell Street, San Francisco, CA, USA
June 29 - July 01, 2011

Robust Rejection of Sinusoids in Stable Nonlinearly Perturbed Unmodelled Linear Systems: Theory and Application to Servo

Vivek Natarajan and Joseph Bentsman, *Member, IEEE*

***Abstract*—Assuming no knowledge of closed-loop dynamics other than being that of a stable nonlinearly perturbed linear system and the forward path gain at the frequency of interest being known and non-zero, a control approach is proposed that rejects a sinusoidal disturbance of known frequency from the system output. The approach consists in partitioning the feedback path of a stable closed-loop system into two weighted paths and inserting between them a loop containing an internal model based filter. The approach is supported by two theorems ascertaining internal stability, that guarantee the rejection of the unwanted sinusoid under the augmentation proposed, with no closed-loop stability loss. The efficacy of the approach is demonstrated through simulations on a model of a servo system consisting of a beam with an electro-hydraulic actuator attached at one end and a mass at the other, and through experiments on the corresponding physical testbed. Robustness of the approach is briefly discussed. A relative non-intrusiveness of the augmentation procedure, a virtual lack of a modeling necessity, and simplicity of estimating the unaugmented forward path gain via experiment on the stable closed-loop system make the approach proposed well suited for industrial use.**

***Index Terms*—Internal model principle, Small gain theorem, Perturbed linear system, Periodic response.**

I. Introduction

TRACKING and rejection of periodic signals with zero steady state error based on internal model principle [1] places the generator of the signal into the stable closed-loop system. This approach has been used widely for both linear and nonlinear plants whose model is known. This paper addresses rejection of an internally generated sinusoid of angular frequency ω_r assuming no knowledge of the plant and hence the closed-loop system, other than that the latter behaves like a stable perturbed linear system and its forward path gain at ω_r, readily found through a closed-loop test, is non-zero. The methodology in [2] for tracking of periodic signals in linear systems uses comparable plant information and could apply to the problem considered here. The novelty of the current work, compared to [2] lies in

i) considering a nonlinearly perturbed linear system. The presence of the nonlinear perturbation is essential as the source of the small amplitude sinusoid to be rejected that dramatically influences the application considered (Sections II, III).
ii) providing a quantitative estimate of stability and disturbance rejection robustness in terms of permissible variations in the forward path gain (Section IV).
iii) using a gain based proof technique which enables visualizing the effect of the small controller parameter that must be tuned in this approach as well as in [2].

The unpartitioned feedback structure is motivated by the repetitive control topology [3]. Experimental and numerical validation of the controller is presented in Section V via magnitude spectrum plots.

II. Application and Problem Statement

In continuous casting of steel, the mold executes a sinusoidal vertical motion of specific frequency and amplitude, imposed by a mold oscillation system. Metallurgical considerations require that the sinusoidal profiles of the mold displacement and velocity be undistorted. The mold oscillation system in some casters consists of a subsystem of beams that supports a heavy mold at one end and is subject to sinusoidal motion by an electro-hydraulic servo actuator with piston attached to this subsystem at the other end, to drive the mold. The servo is open loop unstable and is typically operated under feedback. The desired mold displacement is specified as the actuator piston position reference. Since the beam subsystem is not rigid, there is an inherent mismatch between the displacement and the velocity profiles at the mold and the actuator ends. At most frequencies the mold displacement profile is a scaled but undistorted version of the actuator displacement profile. This problem is easily resolved by suitably scaling the piston reference. However, at frequencies that are submultiples of the first resonant frequency of the beams in the subsystem, a significant distortion is observed in the mold displacement profile. The goal is to identify the source of this submultiples distortion problem and eliminate it.

To carry out experiments, a testbed of the mold oscillation system was built at Nucor Steel, Decatur. The testbed (Fig. 1) has a hinged hollow beam that supports a heavy mass, resembling a mold, on one end and has a servo actuator located at the other end. It exhibits the submultiples phenomenon present in the mold oscillation system, albeit more pronounced. The first resonance frequency of the beam is 9.65 Hz. When the beam is driven by the actuator at 4.8 Hz, the mold displacement profile is severely distorted.

V. Natarajan (email: vnatara2@illinois.edu) and J. Bentsman (corresponding author: Ph: 217-244-1076, Fax: 217-244-6534, email: jbentsma@illinois.edu) are with the Department of Mechanical Science and Engineering, University of Illinois at Urbana-Champaign, IL 61801, USA. This work was supported by NSF grant CMMI-0900138 and by Nucor Steel, Decatur. Glynn Elliott from Nucor Steel, Decatur, is gratefully acknowledged for building the mold oscillation system testbed.

Fig. 2 shows the testbed piston and the mold displacement profiles with servo under proportional feedback with a controller gain 2. The reference to the piston is a sinusoid of 3 mm magnitude and 4.8 Hz frequency. The distortion in the mold displacement is clearly visible, while the piston displacement seems to track the reference perfectly. The magnitude spectrum of the two signals shown in Fig. 3 reveals, however, a small peak of about 0.04 mm at 9.6 Hz, which is twice the reference frequency, in the piston displacement. It was conjectured that being near the beam resonance frequency, this peak - a manifestation of the nonlinear servo dynamics - is amplified by the beam, yielding distortion at the mold end. Experiments verified that when the piston displacement was a sinusoid of 0.05 mm magnitude and 9.65 Hz frequency, the mold displacement magnitude was about 1.5 mm, which matches well the magnitudes of peaks in Fig. 3. It is therefore expected that elimination of sinusoids near resonance frequency in the piston displacement signal will ensure distortion free mold displacement. Hence, the reference and the actual piston displacements are taken to be the input and output, respectively, for controller design in this paper. Since the frequencies near 9.65 Hz have been identified to be the cause of distortions, in the rest of the paper the position signals are not plotted due to space constraints; instead the magnitude spectrum of these signals around 9.65 Hz is presented.

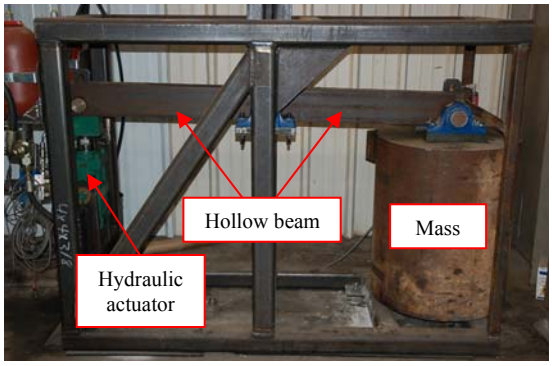

Fig. 1. Picture of the mold oscillation system testbed

Electro-hydraulic servos, though inherently nonlinear, are designed to exhibit stable predominantly linear behavior in a nominal range of operation under feedback, implemented typically in the form of a P or a PI controller [4]. The effect of the beam on the piston in the operating range is mostly linear as well, making a linear system perturbed by small nonlinearity a plausible model for the input-output (reference - actual piston position) behavior of the servo system/testbed. This is confirmed, both in simulations and experiments, by the absence of any large nonlinear effects at the actuator output. Based on the above discussion the following *problem statement* is formulated:

Given a stable closed-loop system exhibiting perturbed linear dynamics that tracks the input sinusoid of frequency ω, but has the output containing small magnitude higher harmonics of ω due to nonlinear effects, augment the loop with a suitable filter so that the harmonic at ω_r in the output is eliminated without affecting the closed-loop stability and the tracking at frequency ω. Here ω_r is a specific integer multiple of ω.

This problem is addressed in Section IV. In the application presented in this paper, ω_r is the first resonance frequency of the beam. The effect of small amplitude higher harmonics at frequencies other than ω_r on the beam is negligible and is omitted from consideration.

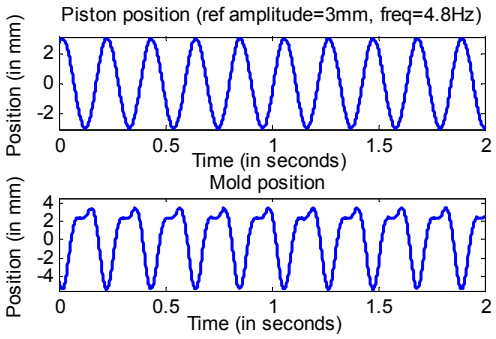

Fig. 2. Experimental result: piston and mold position with piston reference at 4.8 Hz

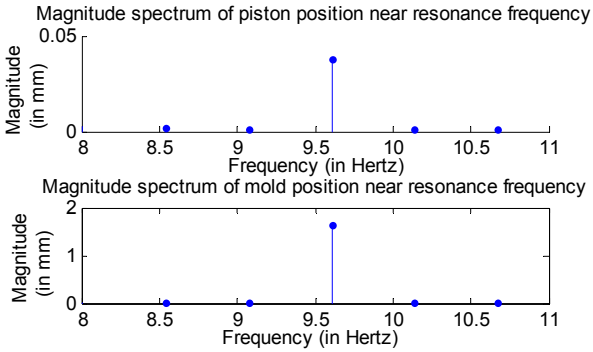

Fig. 3. Experimental result: magnitude spectra of piston and mold position near resonance frequency

III. Coupled Servo-Beam Model and Simulations

A. Electro-hydraulic servo model

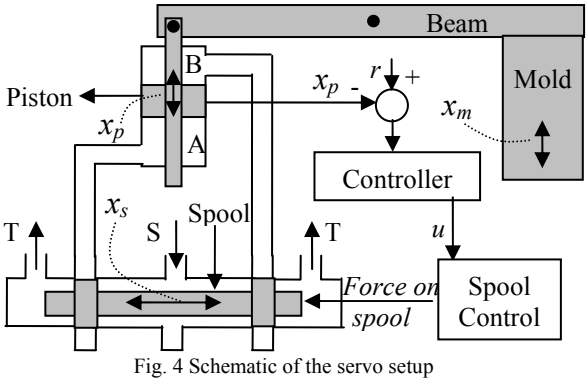

Fig. 4 Schematic of the servo setup

A layout of the coupled servo and beam system is shown in Fig. 4, where 'S' and 'T' refer to the supply of the pressurized fluid and the fluid on the tank side, respectively.

The hydraulic actuator functions as follows. When the spool moves to the right, 'S' is connected to chamber 'B' and the piston is pushed down. When the spool moves to left, 'S' is connected to chamber 'A' and the piston is pushed up. Hence, the appropriate motion of the spool can cause the piston to oscillate. The servo system typically functions in the closed loop. The error between the desired and the actual piston position is used to control the spool position. Piston position x_p is governed by the equation

$$m_p\ddot{x}_p + b\dot{x}_p = (P_A - P_B)a_p - m_p g + F_B \qquad (1)$$

where m_p (2 Kgs), b (1000 N.sec/m), P_A, P_B, a_p (0.0046 m^2), g, F_B stand for the piston mass, damping, pressure in chamber 'A', pressure in chamber 'B', piston area, gravity, and force from the beam, respectively. When x_p is zero, chambers 'A' and 'B' have equal volumes. The pressures in chambers 'A' and 'B' are governed by

$$\begin{aligned} \dot{P}_A &= \beta\left(q_A - a_p\dot{x}_p\right)\Big/\left(V_A + a_p\left(L + x_p\right)\right), \\ \dot{P}_B &= \beta\left(-q_B + a_p\dot{x}_p\right)\Big/\left(V_B + a_p\left(L - x_p\right)\right). \end{aligned} \qquad (2)$$

where β (1.5x10^9 Pa), q_A, q_B, V_A (4.7113x10^{-5} m^3), V_B (7.0464x10^{-5} m^3), L (0.015 m) are bulk modulus of the actuator fluid, flow rates into chamber 'A' and out of chamber 'B', volumes of tubes connected to chambers 'A' and 'B' and half the stroke length of the piston, respectively. Assuming turbulent flow conditions, the flow rates q_A and q_B are given by

$$q_A = \begin{cases} c(d - x_s)\sqrt{P_s - P_A}, & x_s < -d, \\ c(d - x_s)\sqrt{P_s - P_A}, & -d < x_s < d, \\ -c(x_s + d)\sqrt{P_A - P_t}, & \\ -c(x_s + d)\sqrt{P_A - P_t}, & x_s > d, \end{cases} \quad \text{and}$$

$$q_B = \begin{cases} c(d - x_s)\sqrt{P_B - P_t}, & x_s < -d, \\ c(d - x_s)\sqrt{P_B - P_t}, & -d < x_s < d, \\ -c(x_s + d)\sqrt{P_s - P_B}, & \\ -c(x_s + d)\sqrt{P_s - P_B}, & x_s > d, \end{cases} \qquad (3)$$

where c (3x10^{-4}), d (1.27x10^{-6} m), P_s (20684250 Pa), P_t (206840 Pa), x_s are flow coefficient, spool underlap length, supply pressure, tank pressure, and spool position, respectively. In Section V.A modifications to this equation when the pressure difference is small are discussed. The spool position dynamics including the spool control is assumed to be governed by a second order system:

$$\ddot{x}_s + 2\zeta_s\omega_s\dot{x}_s + \omega_s^2 x_s = \omega_s^2 u\,. \qquad (4)$$

Here u is the input generated by a controller using error between x_p and desired reference signal r, as seen in Fig. 4. The value of ζ_s is 0.6 and of ω_s is 255 rad/sec. Typically, a proportional control law

$$u = k\left(x_p - r\right) \qquad (5)$$

is used where k is the proportional gain. In Fig. 4 x_m is the mold position.

B. Beam model

The hollow beam in the testbed is modeled as two beams attached at the hinge, each using Timoshenko beam model consisting of two coupled second order PDEs. The coordinate along the length of the beams is x. The beams are coupled via the boundary conditions at the hinge location $x = 0$ that ensure that the torque and angular displacement at this location are identical. Thus, the model of the hinged beam of length $2l$ (1.76 m) shown in Fig. 5, with the vertical and the angular displacements to the left and to the right of the hinge denoted by (y_L, ψ_L) and (y_R, ψ_R), respectively, is given by a set of 4 coupled PDEs of the form

$$m_b\frac{\partial^2 y_L}{\partial t^2} + \gamma_y\frac{\partial y_L}{\partial t} = \frac{\partial}{\partial x}\left(k'Ga_b\left(\frac{\partial y_L}{\partial x} - \psi_L\right)\right) - m_b g\,,$$

$$\frac{I}{a_b}m_b\frac{\partial^2 \psi_L}{\partial t^2} + \gamma_\psi\frac{\partial \psi_L}{\partial t} = \frac{\partial}{\partial x}\left(EI\frac{\partial \psi_L}{\partial x}\right) + k'Ga_b\left(\frac{\partial y_L}{\partial x} - \psi_L\right),$$

$$m_b\frac{\partial^2 y_R}{\partial t^2} + \gamma_y\frac{\partial y_R}{\partial t} = \frac{\partial}{\partial x}\left(k'Ga_b\left(\frac{\partial y_R}{\partial x} - \psi_R\right)\right) - m_b g\,,$$

$$\frac{I}{a_b}m_b\frac{\partial^2 \psi_R}{\partial t^2} + \gamma_\psi\frac{\partial \psi_R}{\partial t} = \frac{\partial}{\partial x}\left(EI\frac{\partial \psi_R}{\partial x}\right) + k'Ga_b\left(\frac{\partial y_R}{\partial x} - \psi_R\right).$$

The mold dynamics is part of the boundary condition of the right beam at $x = l$. The boundary conditions are

$$y_L(-l) = x_p(t),\ EI\frac{\partial \psi_L(-l)}{\partial x} = 0,\ y_L(0) = 0,\ y_R(0) = 0,$$

$$\psi_L(0) = \psi_R(0),\ EI\frac{\partial \psi_L(0)}{\partial x} = EI\frac{\partial \psi_R(0)}{\partial x},\ EI\frac{\partial \psi_R(l)}{\partial x} = 0,$$

$$k'Ga_b\left(\frac{\partial y_R(l)}{\partial x} - \psi_R(l)\right) + Mg + M\frac{\partial^2 y_R(l)}{\partial t^2} + \gamma_m\frac{\partial y_R(l)}{\partial t} = 0.$$

In the equations m_b (69.256 Kg/m), a_b (0.0088 m^2), G (7.7 x10^{10} Pa), E (2 x10^{11} Pa), I (1.9204 x10^{-5} m^4), γ_y / γ_ψ (10 / 10 Kg/m/sec), γ_m (2), k' (0.83), M (2250 Kgs) stand for mass of beam per unit length, area of cross section of beam, shear modulus, Young's modulus, moment of inertia of beam, beam transverse/angular displacement damping, mold damping, shear constant, and mold mass. The coupling between the nonlinear actuator and the beam is via the piston displacement entering the boundary condition for the left beam and the force F_B from the beam acting on the piston where

$$F_B = k'Ga_b\left(\frac{\partial y_L(-l)}{\partial x} - \psi_L(-l)\right). \qquad (6)$$

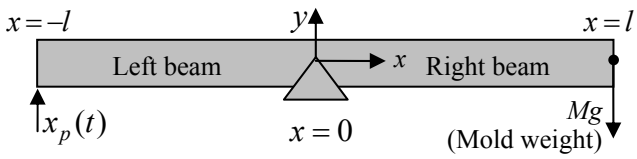

Fig. 5. Beam Schematic

C. Simulation results

Simulation of the servo system in Fig. 4 is performed using the nominal parameter values presented above. The

initial chamber pressures are set at $P_A = P_B = 50\ P_t$. All other initial conditions are zero. The servo simulation uses a proportional controller, with the value of u in eq. (4) given as $u = 0.6\left(x_p - r(t)\right)$ where $r(t)$ is a sinusoid of 3 mm magnitude and 4.8 Hz frequency. The simulated mold position exhibits distortions, similar to those seen in the experiment. These distortions occur due to the nonlinear characteristics of the actuator that gives rise to small amplitude sinusoid of frequency 9.6 Hz in the piston position, which excites the beam resonance. This is confirmed using spectral analysis of the simulated piston and mold position data (Fig. 6). Therefore, the model presented adequately exhibits the submultiples problem and can be used as a platform for testing control strategies.

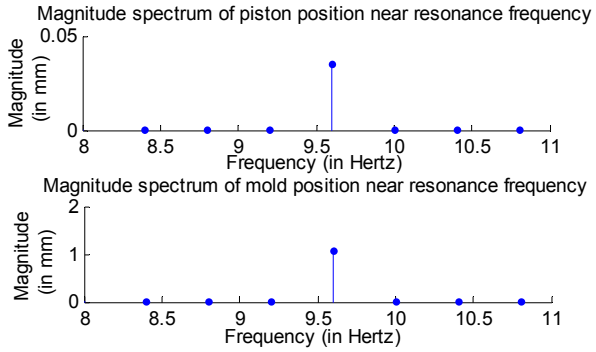

Fig. 6. Simulation result: magnitude spectra of piston and mold position around resonance frequency

IV. Controller Design and Analysis

A. Theorems on controller design

Theorem 1 deals with the topology where the feedback signal is not partitioned (Fig. 7), while Theorem 2 considers the general case (Fig. 9) with weighted partitioned feedback path. To formulate Theorem 1, consider the system shown in Fig. 7, referred to as the unpartitioned unaugmented system, where *P* is a nonlinear plant, *K* is a controller that stabilizes the loop, *r* is the reference input, and *y* is the output.

Theorem 1: Assume that the closed loop system in Fig. 7 is described by a perturbed linear model:

$$\dot{x} = A_{cl}x + B_{cl}u + \varepsilon g(x), \qquad y = C_{cl}x, \qquad (7)$$

where A_{cl} is Hurwitz and $\varepsilon g(x)$ is a small nonlinear perturbation. Also assume the following:

B1. $g(x): \mathbb{R}^n \to \mathbb{R}^n$ is a continuous function, with $g(0) = 0$, such that for any bounded domain $D \subset \mathbb{R}^n$, there exists L such that $\|g(x_1) - g(x_2)\|_n < L\|x_1 - x_2\|_n$, $\forall\ x_1, x_2 \in D$. Let the input r and initial conditions be uniformly bounded. $\|\bullet\|_n$ is the Euclidean norm in $\mathbb{R}^n$.

B2. Assume that the unpartitioned unaugmented system tracks input sinusoid of frequency ω, but its output contains small amplitude higher harmonics of ω, including ω_r, due to nonlinear effects. Here ω_r is an integer multiple of ω.

B3. When the reference input r is a sinusoid of frequency ω_r, the corresponding steady state periodic outputs y_{ss} and (r-y_{ss}) contain sinusoids at that frequency; let they be $S_{y_{ss},\omega_r}(t)$ and $S_{r-y_{ss},\omega_r}(t)$ respectively. Assume that the complex gain g_{KP} from S_{r-y_{ss},ω_r} to S_{y_{ss},ω_r}, referred to as the unaugmented system forward path gain at ω_r, satisfies the condition

$$\left|1/(1+g_{KP})\right| < 1. \qquad (8)$$

Next consider the feedback system shown in Fig. 8, further referred to as the unpartitioned augmented system. Let F be the linear stable transfer function

$$F(s) = \frac{2e\omega_r^{\,2}}{s^2 + 2e\omega_r s + \omega_r^{\,2}} \frac{s - \omega_r}{s + \omega_r} \qquad (9)$$

where $0 < e \ll 1$. For a sufficiently small choice of e, under the above assumptions, if ε is small, the unpartitioned augmented system is stable and tracks the input sinusoid of frequency ω and possibly contains small magnitude higher harmonics of ω induced by the nonlinear perturbation, but the harmonic at frequency ω_r is asymptotically eliminated from its output.

Proof: The proof uses the small gain theorem, a series of block diagram manipulations and periodic response of nonlinearly perturbed systems. Details are omitted for lack of space. It can be shown that, for ε sufficiently small, if

$$F(s)/\left(1 + G(s)\right) \neq 1, \qquad \forall s \in \bar{\mathbb{C}}^+ \cup \{\infty\} \qquad (10)$$

internal stability of the augmented unpartitioned system in Fig. 8 is guaranteed, which in turn guarantees asymptotic elimination of the harmonic at frequency ω_r from its output. Here $\bar{\mathbb{C}}^+$ is the closed right half complex plane and $G(s)$ is the transfer function of the linear system

$$\dot{z} = \left(A_{cl} + B_{cl}C_{cl}\right)z + B_{cl}u, \qquad y = C_{cl}z.$$

For small ε, (10) follows from (8). □

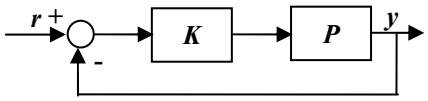

Fig. 7. Block diagram of the unpartitioned unaugmented system

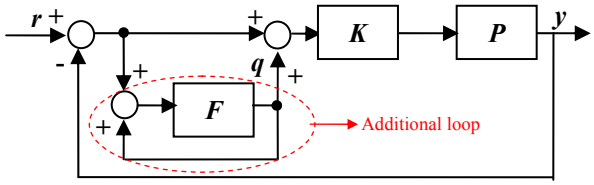

Fig. 8. Block diagram of the unpartitioned augmented system

Remark 1: With (8) *being only a sufficient condition, Theorem 1 can be restated more generally using* (10) *in B3. However, verifying the latter in experiments is not simple.*

When the controller-plant gain at ω_r satisfies neither (8) nor (10), increasing the controller gain and, hence, the forward path gain could possibly result in one of these gain conditions being satisfied to guarantee stability of the unpartitioned augmented loop. This approach is employed to satisfy the gain condition in the experiments with the testbed in Section V.C where a proportional controller is used.

Increasing the controller gains can lead, however, to the unaugmented closed loop stability loss. In this scenario, when controller gains are fixed and gain conditions are not satisfied, a modified feedback structure that provides added flexibility in guaranteeing the stability of the corresponding augmented loop, while solving the problem of Section II, would be required. Such a structure containing a partitioning of the feedback path with a stable filter is introduced in Theorem 2, which generalizes Theorem 1 (Fig. 9). Stability of the augmented loop corresponding to this structure (Fig. 10) is guaranteed by a suitable choice of the partitioning filter as long as the forward path gain at ω_r is non-zero. In the production unit, increasing gains to a desired value may not be feasible and Theorem 2 could prove valuable.

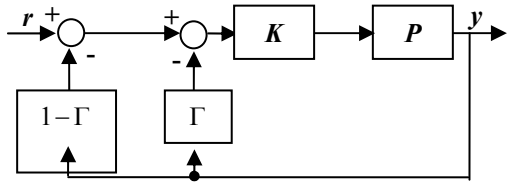

Fig. 9. Block diagram of partitioned unaugmented system with stabilizing feedback

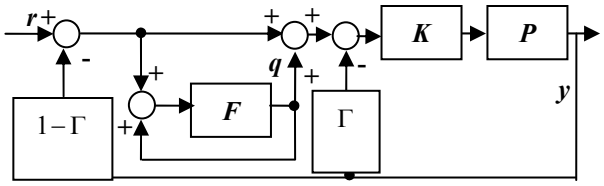

Fig. 10. Block diagram of partitioned augmented system

Theorem 2: Consider the feedback system shown in Fig. 9, referred to as the partitioned unaugmented system where P, K, r, and y are as in Theorem 1 and Γ *is a stable filter to be chosen. Assume that this system is described by the perturbed linear system (7) with* A_{cl} *Hurwitz and* $\varepsilon g(x)$ *being a small nonlinear perturbation. Let assumptions B1 and B2 hold. Let* g_{KP}*, as defined in B3, be non-zero and choose* Γ *such that* $\Gamma(j\omega_r) = -1/g_{KP}$*. Consider the feedback system in Fig. 10, referred to as the partitioned augmented system where* F *is given by* (9)*. For a sufficiently small choice of e, under the above assumptions, for sufficiently small* ε*, the partitioned augmented system is stable and tracks the input sinusoid of frequency* ω *and possibly contains small magnitude higher harmonics of* ω *induced by the nonlinear perturbation, but the harmonic at frequency* ω_r *is asymptotically eliminated from its output.*

Proof: It can be shown that with G as in the proof of Theorem 1, the condition for the stability of the partitioned augmented loop instead of (10), takes the form

$$F(s).\big(1+\Gamma(s)G(s)\big)/\big(1+G(s)\big) \neq 1, \quad \forall s \in \bar{\mathbb{C}}^{+} \cup \{\infty\}, \qquad (11)$$

which holds if

$$\big(1+\Gamma(j\tau)G(j\tau)\big)/\big(1+G(j\tau)\big) < 1/F(j\tau), \ \forall \tau \in \mathbb{R} \cup \{\infty\}, \qquad (12)$$

which in turn follows, for sufficiently small ε, from the choice $\Gamma(j\omega_r) = -1/g_{KP}$ and properties of F. □

B. Robustness of the controller

Given a stable plant, Theorem 2 proposes an internal model based controller to reject an internally generated sinusoidal disturbance. The sole measurement used in this approach is the forward path gain at the frequency of interest, g_{KP}. In practice, the actual forward path gain could change from g_{KP} to $g_{KP} + \Delta g_{KP}$, owing to changes in the plant. It is useful to obtain conditions on $|\Delta g_{KP}|$ which guarantee that even when the forward path gain changes, the stability and disturbance rejection performance of the augmented loop in Fig. 10 which was designed using g_{KP}, is unaffected. Such a condition can be obtained using (12). Since the nonlinear perturbation is small, $|g_{KP} - G(j\omega_r)|$ is small. It can be shown that any Δg_{KP} that satisfies $|\Delta g_{KP}|/\big(|g_{KP}||1 + g_{KP} + \Delta g_{KP}|\big) < 1$ is a permissible variation and the augmented loop stability is not affected. Using this estimate inequality bounds on $|\Delta g_{KP}|$ can be obtained and used in combination with experimental monitoring of the changes in g_{KP} to estimate the risk of instability. For example, if $g_{KP} = 1$, then any Δg_{KP} with $|\Delta g_{KP}| < 1$ is permissible. The unaugmented loop is assumed to be stable.

V. Numerical and Experimental Controller Validation

A. Properties of the nonlinearities in servo system

The input-output dynamics of the testbed (Section II) can be captured by a perturbed linear model (7) with small ε. The simplified model (3) for the orifice flow is in terms of a non-Lipschitz at zero square root of the pressure drop. Since orifice flow is better captured by a more complex Lipschitz function [5], that equals (3) for pressure drops not near zero and since the simulated pressure drops are always bounded away from zero, it is reasonable to assume that a Lipschitz function $g(x)$ in (7) captures the flow nonlinearities making Theorems 1 and 2 applicable to the model (1)-(6).

B. Numerical controller validation

The unpartitioned control configuration of Theorem 1 is applied to the computational model of the testbed, presented in Sections III.A and III.B to eliminate the distortions in the simulated mold position. To verify the validity of assumption *B3*, the reference is chosen to be a sinusoid at frequency 9.65 Hz and magnitude 0.05 mm, and $|1/(1+g_{KP})|$

is calculated. As in Section III, a proportional controller with a gain of 0.6 is used and simulations indicate that $\left|1/(1+g_{KP})\right|<1$. To test the scheme, $r(t)$ is chosen to be a sinusoid of magnitude 3 mm and frequency 4.8 Hz. A filter is introduced as in Theorem 1 with $\omega_r = 2\pi \times 9.65$ and $e = 0.1$ in (9). The piston position signals (not presented here) before and after augmentation are similar, indicating that the augmentation of the closed loop has minimal effect on its tracking at 4.8 Hz, as stated in Theorem 1. Furthermore, the distortion in the mold position is dramatically reduced owing to the drastic reduction of the magnitude of sinusoid at frequency 9.6 Hz contained in piston position which in turn reduces the corresponding magnitude in the mold position (please, compare Fig. 11 and Fig. 6).

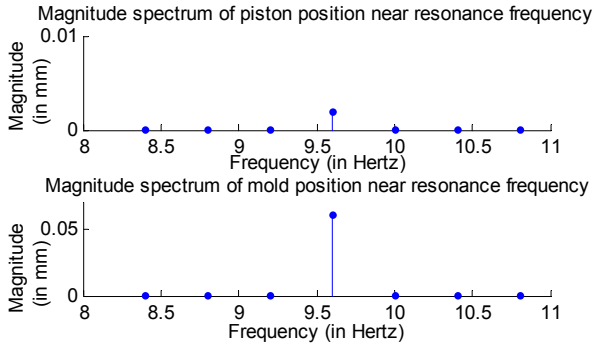

Fig. 11. Simulation result: Magnitude spectra of piston and mold position near resonance frequency with augmented closed loop (magnitude at 9.6 Hz in mold position is reduced by a factor of 17 compared to Fig. 6)

C. *Experimental controller validation*

The controller validation was carried out in three steps. In step one, the estimate of g_{KP} at ω_r for the unaugmented system under proportional feedback with a gain 2 (i.e. *k=2*) considered in Section II was obtained using a reference input of frequency 9.65 Hz and magnitude 0.05 mm. The corresponding gain g_{KP} did not satisfy the conservative condition (8), and controller gain increase to 4 or 5 was required to obtain $\left|1/(1+g_{KP})\right|<0.7$, guaranteeing augmented system stability. To retain controller gain 2, Theorem 2 could have been applied. This, however, was not pursued, since according to Remark 1, verification of (8) was only sufficient, and internal stability of the unpartitioned augmented system with controller gain 2 was attainable if (10), but not necessarily (8), were satisfied. This provided guidance for the next two steps.

In step two, the augmented loop was tested in a wide frequency range: first, the proportional gain was set at 1, and the reference was chosen to be a sinusoid of 1 mm magnitude and 1 Hz frequency, resulting in unexpected oscillations. Increasing the proportional gain to 2, although not satisfying (8) as indicated above, permitted the augmented system to be operated safely over all amplitudes and frequencies of interest, apparently satisfying condition (10) and making further gain increase unnecessary.

Step three demonstrated the efficacy of the controller: the reference input was chosen to be a sinusoid of magnitude 3 mm and frequency 4.8 Hz and the servo proportional feedback gain was set at 2, all as in Section II where large mold displacement distortion was observed. The filter parameters were $\omega_r = 2\pi \times 9.65$ and $e = 0.1$. From Fig. 12, it is seen that the magnitude of the sinusoid at 9.6 Hz present in the piston position, and hence the mold position, is significantly reduced, compared to Fig. 3, leading to a significant reduction in the distortion in the mold position that was observed in the unaugmented case (Fig. 2). The piston position signals (not shown here) before and after augmentation are similar, since the augmentation of the closed loop has minimal effect on its tracking at 4.8 Hz. In Fig. 12, the small peaks around 9.6 Hz are artifacts of data processing invisible in case of simulations and in Fig. 3 due to much larger sampling rate and larger x-axis scale, respectively.

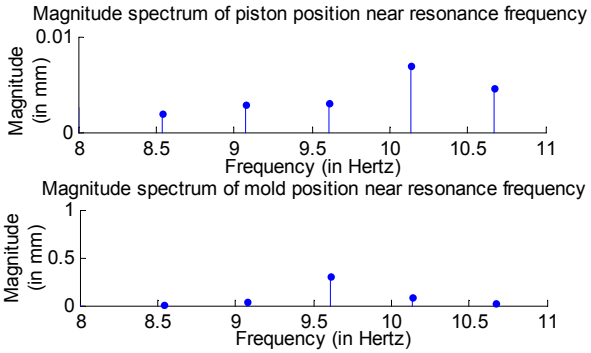

Fig. 12. Experimental result: magnitude spectra of piston and mold position around resonance frequency after loop augmentation (magnitude at 9.6 Hz in mold position is reduced by a factor of 5 compared to Fig. 3)

REFERENCES

[1] B. A. Francis and W. M. Wonham, "The internal model principle for linear multivariable regulators," *Appl. Math. Optim.*, Vol. 2, No. 2, pp. 170-194, 1975.

[2] E. J. Davison, "Multivariable tuning regulators: The feedforward and robust control of a general servomechanism problem," *IEEE Transactions on Automatic Control,* Vol. 21, No. 1, pp. 35-47, 1976.

[3] S. Hara, Y. Yamamoto, T. Omata and M. Nakano, "Repetitive control system: A new type servo system for periodic exogenous signals," *IEEE Transactions on Automatic control*, Vol. 33, No. 7, pp. 659-668, 1988.

[4] D. H. Kim and T-C. Tsao, "A linearized electrohydraulic servovalve model for valve dynamics sensitivity analysis and control system design," *ASME Journal of Dynamic Systems, Measurement, and Control*, Vol. 122, pp. 179-187, 2000.

[5] W. Borutzky, B. Barnard and J. Thoma, "An orifice flow model for laminar and turbulent conditions," *Simulation Modelling Practice and Theory,* Vol.10*,* pp. 141-152, 2002.